Proteomics-Based Safety Evaluation of Multi-Walled Carbon Nanotubes

Hisao Haniu [a,*], Yoshikazu Matsuda [b], Kenji Takeuchi [c], Yoong Ahm Kim [c], Takuya Hayashi [c] and Morinobu Endo [c]

[a] School of Medicine, Shinshu University, 3-1-1 Asahi, Matsumoto, Nagano 390-8621, Japan

[b] Department of Pathophysiology, Nihon Pharmaceutical University, 10281 Komuro, Ina-machi, Saitama 362-0806, Japan

[c] Faculty of Engineering, Shinshu University, 4-17-1 Wakasato, Nagano-shi, Nagano 380-8553, Japan

[*] To whom correspondence should be addressed:

Hisao Haniu, Institute of Carbon Science and Technology, Shinshu University, School of Medicine

3-1-1 Asahi, Matsumoto, Nagano 390-8621, Japan

Tel: +81-263-37-2659, Fax: +81-263-35-8844

E-mail: hhaniu@shinshu-u.ac.jp

This study evaluated the biological responses to multi-walled carbon nanotubes (MWCNTs). Human monoblastic leukemia cells (U937) were exposed to as-grown MWCNTs and MWCNTs that were thermally treated at 1800 °C (HTT1800) and 2800 °C (HTT2800). Cell proliferation was highly inhibited by as-grown but not HTT2800. However, both as-grown and HTT1800, which include some impurities, were cytotoxic. Proteomics analysis of MWCNT-exposed cells revealed 37 protein spots on 2-dimensional electrophoresis gels that significantly changed ($p < 0.05$) after exposure to HTT1800 with a little iron and 20 spots that changed after exposure to HTT2800. Peptide mass fingerprinting identified 45 proteins that included heat shock protein β-1, neutral α-glucosidase AB, and DNA mismatch repair protein Msh2. These altered proteins play roles in metabolism, biosynthesis, response to stress, and cell differentiation. Although HTT2800 did not inhibit cell proliferation or cause cytotoxicity in vitro, some proteins related to the response to stress were changed. Moreover, DJ-1 protein, which is a biomarker of Parkinson's disease and is related to cancer, was identified after exposure to both MWCNTs. These results show that the cytotoxicity of MWCNTs depends on their impurities, such as iron, while MWCNTs themselves cause some biological responses directly and/or indirectly *in vitro*. Our

proteomics-based approach for detecting biological responses to nanomaterials is a promising new method for detailed safety evaluations.

Keywords: carbon nanotubes, safety evaluation, proteomics, protein expression, *in vitro*

Abbreviations:

CNT: carbon nanotube; 2-DE: 2-dimentional gel electrophoresis; GO: gene ontology; β-ME: β-mercaptoethanol; MWCNT: multi-walled carbon nanotube; PMF: peptide mass fingerprinting; SDS: sodium dodecyl sulfate; TFA: trifluoroacetic acid

Introduction

Nanomaterial technology, such as sp^2-based carbon nanotubes (CNTs), has been developed during this century. The nanoscale size and extraordinary physicochemical properties of CNTs are very useful in applications such as in nanocomposites, sensors, energy storage, energy-conversion systems, field-emission displays, radiation sources, medical applications and other nanodevices (Endo *et al.*, 2008; Usui *et al.*, 2008). CNTs can be mass produced by the chemical vapor deposition method, especially the floating reactant method (Endo, 1988). Simultaneously, the occupational and public exposure to manufactured nanomaterials has increased significantly. Although biocompatibility is usually better in carbon materials, CNTs possess a unique nanoscale size and a high aspect ratio (above 100); thus, CNTs, like asbestos, may yield extraordinary hazards to human health (Borm *et al.*, 2006; Nel *et al.*, 2006; Kostarelos, 2008).

The human body can be exposed to CNTs through five possible routes: inhalation of airborne CNTs, dermal penetration by skin contact, injection of engineered CNTs, implantation of composited CNTs, and ingestion of drinking water or food additives. Safety evaluations of CNTs have been performed with *in vitro* and *in vivo* models. In *in vivo* experiments, the pulmonary toxicity of CNTs was evaluated by intratracheal instillation, and the carcinogenicity of CNTs such as asbestos was tested by intraperitoneal injection into rats or mice (Muller *et al.*, 2005; Inoue *et al.*, 2008; Poland *et al.*, 2008; Takagi *et al.*, 2008). These experiments found that CNTs can induce inflammation, fibrosis, and granulomas in the lungs and that CNTs have a carcinogenic effect in the abdominal cavity. *In vitro* experiments evaluated the effects of CNTs on lung epithelial cells, keratinocytes, and immune cells such as macrophages

(Monteiro-Riviere *et al.*, 2005; Kagan *et al.*, 2006; Sarkar *et al.*, 2007; Hirano *et al.*, 2008; Jacobsen *et al.*, 2008; Herzog *et al.*, 2009; Yang *et al.*, 2009). These studies found that CNTs might be cytotoxic and induce cytokine production or oxidative stress. However, some reports have found that CNTs did not cause any significant biological responses (Flahaut *et al.*, 2006; De Nicola *et al.*, 2007; Pulskamp *et al.*, 2007; Yang *et al.*, 2008). The conflicting results may be caused by differences in the type of CNTs (diameter, length, single-walled or multi-walled), exposure amount, exposure period, and dispersion medium. Another important factor is the influence of the impurities included in CNTs, especially the iron that is used as a catalyst during CNT production. In fact, the carcinogenic potency of asbestos is increased by iron, which accelerates the generation of oxygen radical species (Gulumian and van Wyk, 1987; Jiang *et al.*, 2006).

Recently, we have proposed a proteomics-based method to evaluate the safety of nanomaterials (Haniu *et al.*, 2009). This method is an attempt to predict delayed toxicity or chronic toxicity by comparing the altered proteins in cultured cells which closely related CNTs-exposure tissues with a database of known disease-related proteins.

In the present study, we used a proteomics approach to evaluate the effects of multi-walled CNTs (MWCNTs) on the protein expression in U937 cells, which can differentiate into macrophages when exposed to a differentiation-inducing agent. We also examined alterations in the expression pattern of intracellular proteins depending on differences in the impurities within the nanotubes by thermally treating highly contaminated as-grown tubes at 1800 °C and 2800 °C in argon.

Materials and methods

Materials

MWCNTs were synthesized in a vertical tubular reactor, via the floating reactant method, using an organic metallic compound (e.g., ferrocene) as a catalyst precursor, toluene as a carbon feedstock, and hydrogen as a carrier gas in a semi-continuous system (Oberlin *et al.*, 1976; Endo, 1988). Benzene solution containing an organic metallic compound was fed into the reactor using a micro-feeding pump. The reaction was performed at 1200 °C to obtain as-grown MWCNTs. Then, we performed high-temperature thermal treatment of as-grown tubes at 1800 °C (HTT1800) and 2800 °C (HTT2800) for 30 min using a graphite resistance furnace in argon (Table 1). The three grades of MWCNTs (e.g., as-grown, HTT1800 and HTT2800) were sterilized with ethylene oxide gas overnight, suspended with 10% gelatin, and sonicated with a water-bath sonicator for 2 h. Before use, the suspended materials were heated at 40 °C and mixed vigorously.

Cell culture and MWCNT exposure

The U937 human monoblastic leukemia cell line was purchased from Riken (Ibaraki, Japan) and grown in an RPMI 1640 medium supplemented with 10% heat-inactivated fetal bovine serum at 37 °C in a 5% CO_2 atmosphere. The cells were seeded at 5×10^4 cells/ml and split approximately twice per week. Fifty microliters of MWCNTs (10 mg/ml) was added to 5 ml of culture medium that contained 2.5×10^5 cells. The same volume of 10% gelatin was added to culture medium as a control. The cells were counted at 24-h intervals and a cytometer was used to determine the cell proliferation rate. We did not use the MTT assay or other spectroscopic analyses to determine cell

proliferation because carbon nanotubes interact with these dyes (Casey *et al*. 2007). The cells were stained with trypan blue dye to assess cytotoxicity.

Preparation of samples for proteomic analysis

The U937 cells cultured with MWCNTs for 96 h were centrifuged, washed 3 times with 250 mM saccharose in 10 mM Tris-HCl (pH 7.0) and solubilized by lysis solution containing 7 M urea, 2 M thiourea, 4% CHAPS, 5% *β*-mercaptoethanol (*β*-ME), and 0.5% IPG buffer (pH 3-10; Bio-Rad, Hercules, CA). The cells were ground with a mini-grinder for 1 min on ice and then sonicated for 10 min at 10 °C in a water-bath sonicator. The samples were centrifuged at 21,600 *g* for 15 min at 10 °C. The supernatant was transferred to a new microtube and kept at -80 °C until use. The protein concentration was determined using a protein assay solution (Bio-Rad).

Two-dimensional gel electrophoresis (2-DE) and image analysis

After rehydration of IPG strips (11 cm, nonlinear pH 3-10; Bio-Rad) overnight at room temperature, 200 μg of protein was loaded onto each strip. Isoelectric focusing was performed by a program of progressively increasing voltage for a total of 30,000 V-h with cooling at 15 °C. The focused IPG strips were then equilibrated for 30 min with slow shaking in an equilibration solution containing 2% sodium dodecyl sulfate (SDS), 16.7 mM Tris-HCl (pH 6.8), 10% glycerol and 5% β-ME. The equilibrated IPG strips were laid on the second dimension gels (12% SDS-polyacrylamide gels; 13.8 cm × 12 cm × 1 mm) and a current of 20 mA was applied for 6 h. Each gel was then fixed in a solution of 50% methanol and 10% acetic acid for a minimum of 30 min and stained for a minimum of 60 min with Quick-CBB (Wako, Osaka, Japan). Gels were destained

with distilled water overnight and then sandwiched between cellophane soaked in 5% methanol and 5% glycerol and scanned with a transmission scanner (CanoScan 9950F; Canon, Tokyo, Japan) at a resolution of 300 dpi. The scanned gel images were analyzed with PDQuest Advanced software (Bio-Rad, version 8.0) to quantify the protein spots. Four sets (n = 4) of independent 2-DE gel analyses were conducted and averaged. We selected the protein spots with more than a two-fold expression change compared to the protein spots of the control.

Protein identification by MALDI-TOF MS

In-gel digestion of 2-DE gel spots was performed as previously described (Haniu *et al.*, 2006). Briefly, protein spots excised from the 2-DE gel were destained with 100 mM ammonium bicarbonate in 50% acetonitrile. The gel pieces were dried and digested with sequencing-grade modified trypsin (Promega, Madison, WI). The peptide solution was recovered, and residual peptide was extracted by shaking with 5% trifluoroacetic acid (TFA) in 50% acetonitrile. The combined solution was concentrated using a lyophilizer. The tryptic peptides dissolved in 0.2% TFA were mixed with a matrix solution (α-cyano-4-hydroxycinnamic acid 10 mg/ml in 50% acetonitrile/0.1% TFA) and applied to a target plate. MS spectra were obtained by MALDI-TOF MS (Voyager Elite, Applied BioSystems, Foster City, CA). The MS spectra were analyzed in the positive-ion mode. The peptide mass fingerprinting (PMF) search was performed through MASCOT (http://www.matrixscience.com) using the NCBInr database. The PMF search parameters were: animal species, *Homo sapiens*; enzyme specificity, trypsin (maximum missed cleavage = 1); modification, propionamide (cysteine), *N*-acetyl (protein), oxidation (methionine), and pyro-glutamate (N-terminal glutamate

and glutamine); and mass tolerance, 0.5 Da. Protein identification was based on the combination of the probability-based MOWSE score for PMF. We declared protein identities based on the criteria that the probability-based PMF MOWSE score exceeds 65 ($p < 0.05$). The identified proteins were categorized according to three ontological aspects using the Generic Gene Ontology (GO) TermMapper (http://go.princeton.edu/cgi-bin/GOTermMapper) (Boyle *et al.*, 2004).

Statistical analysis

Unpaired two-tailed Student's *t*-tests were used for the statistical analyses of the differences in cell count data and raw quantitative data for each protein spot on the 2-DE gels. *P* values of 0.05 or less were considered statistically significant.

Results

Cell proliferation

Although U937 cells have the capacity to differentiate into macrophage-like cells when treated with a differentiation-inducing agent (e.g., phorbol 12-myristate 13-acetate), MWCNT exposure did not induce differentiation. Figure 1 illustrates the cell proliferation in the control group and the MWCNT-exposed groups. U937 cells treated with as-grown showed a significant suppression in cell proliferation ($p < 0.05$) at 24, 72 and 96 h compared with the control and at 72 and 96 h compared with HTT2800. On the other hand, HTT1800- and HTT2800-exposed U937 cells tended to have suppressed proliferation, but the suppression was not statistically significant except for the suppression at 48 h mediated by HTT1800.

Cytotoxic assay

Cells stained by trypan blue were observed at 48 h, and they appeared to contain phagocytosed MWCNTs (Fig. 2). Many trypan blue-stained cells exposed to as-grown or HTT1800 contained asbestos-like bodies. Cells exposed to HTT2800 were adhered on MWCNTs, but most of the cells were not stained. After 48 h, there was no distinctive change in cytotoxicity.

Two-dimensional gel electrophoresis

Two-DE was used to investigate the altered expression of proteins in U937 cells exposed to MWCNTs for 96 h. We could not obtain a proteome map from the as-grown group because the as-grown strongly suppressed cell proliferation. Representative images of the proteome map of each group are shown in Fig. 3a~c. The images obtained from running electrophoresis four times for each group contained a total of more than 700 protein spots. To determine expression differences, the quantity among all matched spots was compared with the control. A comparison between the control and HTT1800-exposed cells yielded 37 protein spots with a two-fold or greater change in expression level and quantitatively significant differences ($p < 0.05$), while a comparison between the control and HTT2800-treated cells yielded 20 protein spots. Of the 37 spots on the HTT1800 gels, 18 were up-regulated and 19 were down-regulated. In the HTT2800 gels, 8 of the 20 spots were up-regulated, and 12 spots were down-regulated. Seven of the significantly changed spots were common to both HTT1800 with HTT2800 gels, and most of the other spots were in the same pattern in

both types of gels. However, some spots in the HTT2800 gels were more greatly changed than in the HTT1800 gels.

Protein identification by PMF

The altered protein spots were cut from the gels and subjected to PMF. Forty-five proteins were identified. These proteins are illustrated by spot number in Fig. 3 and listed accordingly in Table 2. The listed proteins were categorized into 17 groups according to their ontological characteristics using GO TermMapper (Table 3). Many of the proteins on the HTT1800 gels were related to the nucleic acid metabolic process, transport, cell death, cell proliferation and transcription. On the other hand, almost equal numbers of proteins related to carbohydrate and protein metabolic process and translation were identified on the HTT1800 and HTT2800 gels.

Discussion

In this study, we investigated the *in vitro* biological responses of cells to three grades of MWCNTs (e.g., as-grown, HTT1800 and HTT2800) with different purities. Table 1 shows the physicochemical properties of these MWCNTs. The proliferation of U937 cells exposed to as-grown was suppressed by more than 50% at 96 h. As-grown contains a lot of iron, polycyclic aromatic hydrocarbons (PAHs), and disordered carbons as compared to HTT1800 and HTT2800. These impurities are inevitable in catalytically grown CNTs. Therefore, it is important to determine if these impurities have toxic effects. Disordered carbons are the same as carbon black from the view point of microtexture (Donnet *et al.*, 1993). That is, disordered carbons are thought to yield a biological response that is similar to that of carbon black. Carbon black is usually used

as a negative control and does not exhibit significant toxicity (Bottini *et al.*, 2006). In our previous report, carbon black did not suppress U937 cell proliferation (Haniu *et al.*, 2009). In the present study, HTT1800 and HTT2800 did not inhibit cell proliferation. The iron and PAHs in HTT1800 and HTT2800 were removed by thermally treating as-grown tubes at temperatures greater than 1800 °C in argon. Iron and PAHs have been reported to contribute to the oxidation reaction (Baulig *et al.*, 2003; Kagan *et al.*, 2006; Guo *et al.*, 2007; Byrne and Baugh, 2008; Liu *et al.*, 2008). Thus, we thought that the impurities (iron and PAHs) in MWCNTs cause the inhibition of cell proliferation. These impurities were removed by thermal treatment; in fact, MWCNTs treated at temperatures greater than 1800 °C did not inhibit cell proliferation. There were no apparent differences between HTT1800 and HTT2800 except for the iron content. The remaining iron consisted of pure iron and iron oxide in HTT1800, while HTT2800 contained ca. 20 ppm of iron. This residual iron may cause cytotoxicity accompanied by a positive reaction with trypan blue. Choi *et al.* (2009) reported that iron oxide caused cell death associated with membrane damage, which is consistent with our result that no cells exposed to HTT2800 were stained by trypan blue.

We obtained 2-DE images from U937 cells exposed to HTT1800 or HTT2800 and control cells; we could not test the as-grown nanotubes group because it contained too many dead cells. To raise the biological reliability of our proteomics data, we extracted only the proteins with expression levels that had changed by more than two-fold and that were significantly different ($p < 0.05$) as compared to the control. As a result, we extracted 50 protein spots, 45 of which were identified by PMF. The expression levels of 35 of these proteins were significantly changed by HTT1800 exposure, and the expression levels of 16 proteins were significantly changed by HTT2800 exposure. Six

proteins with more than two-fold change and statistical significance were common to both HTT1800 exposure and HTT2800 exposure, and an additional 8 proteins with only a statistically significant difference were common to both MWCNTs. The exact mechanism responsible for the changes in the expression levels of these 14 proteins is not clear. It is thought that the direct interaction of the cells with MWCNTs and CNTs induces indirect cytotoxicity (Casey *et al.*, 2008; Guo *et al.*, 2008). Guo *et al.* found that SWCNTs adsorb folate and that the resulting folate deficiency reduces viability. Moreover, a proteomics analysis of cells cultured without folate (Duthie *et al.*, 2008) identified 13 proteins that correspond with our results. Nine of these 13 proteins are contained in the group of 14 proteins that are common to HTT1800 and HTT2800 exposure. We must carefully distinguish the direct influences of CNTs from their indirect influences and consider that the CNTs with such nutriment absorption ability are phagocytosed by the cell (Jin *et al.*, 2009). It is possible that unknown factors are responsible for the remaining protein differences in cells exposed to HTT2800 (Warheit, 2006). One factor may be the size of aggregated MWCNTs (Soto *et al.*, 2007). Although our three grades of MWCNTs have very similar physical and chemical properties, their dispersal states in culture medium are apparently different. With increasing thermal-treatment temperatures, the size of the aggregated MWCNTs decreases (data not shown).

According to the ontological characteristics used by GO TermMapper, many proteins related to metabolism were contained in the group of 14 proteins common to HTT1800 and HTT2800. The functions of these metabolism proteins are: signal transduction/cell communication, response to stress, transport, cell differentiation, cell cycle and cell death. It is noteworthy that there are proteins related to the response to stress or cell

death that are altered in the HTT2800 group without the suppression of cell proliferation or the induction of cytotoxicity, whereas the proteins that function in cell proliferation and transcription were changed only in the case of HTT1800. In particular, the remarkable differences in interferon-induced protein 53 and calreticulin after HTT1800 exposure and HTT2800 exposure may promote cell proliferation. Heat shock protein 60 induces the production of cytokines that were induced by CNT exposure in previous reports (Cohen-Sfady *et al.*, 2005; Witzmann and Monteiro-Riviere, 2006; Osterloh *et al.*, 2007; Shvedova *et al.*, 2007; Shvedova *et al.*, 2008a; Shvedova *et al.*, 2008b). Thus, our proteomics approach can detect intracellular changes with great sensitivity, which may allow us to predict slowly progressing diseases.

Protein DJ-1 (DJ-1) is significantly decreased in both the HTT1800 and HTT2800 groups. According to the Swiss-Prot database, DJ-1 may act as a redox-sensitive chaperone and as a sensor for oxidative stress, and it may protect neurons against oxidative stress and cell death. Moreover, DJ-1 is a biomarker in Parkinson's disease (Kubo *et al.*, 2006; Wood-Kaczmar *et al.*, 2006). Although the HTT2800 contained almost no iron, DJ-1 was down-regulated more than in HTT1800, which contains a small amount of iron. We previously found that carbon black, which contains the same type of carbon as CNT, did not change DJ-1 expression (Haniu *et al.*, 2009). Petrak et al. (2006) have reported that iron overload in human hepatoma cells did not significantly change DJ-1 expression. These results led to the conclusion that DJ-1 expression was not decreased by the iron oxidative stress, and the authors suggested the possibility that direct contact between U937 cells and MWCNTs causes a reduction in the level of DJ-1. DJ-1 appears to play an important role in carcinogenesis in breast cancer, non-small cell lung carcinoma and prostate cancer (Le Naour *et al.*, 2001; MacKeigan *et al.*, 2003;

Hod, 2004). The DJ-1 expression level is up-regulated in most kinds of cancer cells. In contrast, our results show the down-regulation of DJ-1. It is possible that an anti-cancer drug could be developed by clarifying the mechanism responsible for the CNT-mediated suppression of DJ-1 expression, although it is necessary to confirm this change in normal cells because we studied a tumor cell line. In this study, the exact function of DJ-1 in the U937 human monoblastic leukemia cell line is not clear. Thus, future studies should examine if CNTs influence neurons.

Witzmann and Monteiro-Riviere (2006) have previously used a proteomic approach to study the biological response of human keratinocytes to MWCNTs. They identified altered expression patterns of 36 proteins after 24-h exposure to MWCNTs and altered expression patterns of 106 proteins after 48-h exposure. Seven of these proteins, including proteasome subunit β type-1, annexin A2, heat shock 27-kDa protein 1, heat shock 70-kDa protein 5, and calreticulin precursor, were also changed in the present study, although the origin of the cells and the exposure times were different. Interestingly, the majority of the 7 proteins were significantly changed in only HTT1800, and most of the 7 proteins are related to response to stress and cell death. The sensitivity of the method used in the previous study to measure iron content is lower than that of our method. Thus, we speculated that their MWCNTs contained a small amount of iron and that the toxicity of the iron contributed to their results. This result suggests the possibility that impurities in the material can be detected by measuring the biological response with a proteomic approach.

In the present study, we performed a comprehensive, proteomics-based analysis of the biological response to nanomaterials in order to obtain safety information. Protein matching will be an efficient method to evaluate the possibility of whether MWCNTs

cause disease, if the protein database related to all diseases is established, like the gene database related to genomic disease. To contribute to the protein database, we are gathering data regarding the changes in protein expression caused by exposing cells to various compounds. At the same time, we are verifying the biological response using a proteomics approach *in vivo*. These data will allow us to assess safety issues regarding CNTs and other nanomaterials in a more accurate way. In addition, the proteomics-based approach is likely to detect impurities, secondary influence, and response mechanism.

Acknowledgements

This research was supported by CLUSTER (the second stage) of Ministry of Education, Culture, Sports Science and Technology, Japan. We are thankful to Professor Shozo Koyama for his strong support and encouragement.

References

Baulig, A., Garlatti, M., Bonvallot, V., Marchand, A., Barouki, R., Marano, F., Baeza-Squiban, A., 2003. Involvement of reactive oxygen species in the metabolic pathways triggered by diesel exhaust particles in human airway epithelial cells. Am. J. Physiol. Lung Cell Mol. Physiol. 285, L671-679.

Borm, P.J., Robbins, D., Haubold, S., Kuhlbusch, T., Fissan, H., Donaldson, K., Schins, R., Stone, V., Kreyling, W., Lademann, J., Krutmann, J., Warheit, D., Oberdorster, E., 2006. The potential risks of nanomaterials: a review carried out for ECETOC. Part. Fibre Toxicol. 3, 11.

Bottini, M., Bruckner, S., Nika, K., Bottini, N., Bellucci, S., Magrini, A., Bergamaschi, A., Mustelin, T., 2006. Multi-walled carbon nanotubes induce T lymphocyte apoptosis. Toxicol. Lett. 160, 121-126.

Boyle, E.I., Weng, S., Gollub, J., Jin, H., Botstein, D., Cherry, J.M., Sherlock, G., 2004. GO::TermFinder--open source software for accessing Gene Ontology information and finding significantly enriched Gene Ontology terms associated with a list of genes. Bioinformatics 20, 3710-3715.

Byrne, J.D., Baugh, J.A., 2008. The significance of nanoparticles in particle-induced pulmonary fibrosis. Mcgill J. Med. 11, 43-50.

Casey, A., Herzog, E., Davoren, M., Lyng, F.M., Byrne, H.J., Chambers, G., 2007. Spectroscopic analysis confirms the interactions between single walled carbon nanotubes and various dyes commonly used to assess cytotoxicity. Carbon 45, 1425-1432.

Casey, A., Herzog, E., Lyng, F.M., Byrne, H.J., Chambers, G., Davoren, M., 2008. Single walled carbon nanotubes induce indirect cytotoxicity by medium depletion in A549 lung cells. Toxicol. Lett. 179, 78-84.

Choi, S.J., Oh, J.M., Choy, J.H., 2009. Toxicological effects of inorganic nanoparticles on human lung cancer A549 cells. J. Inorg. Biochem. 103, 463-471.

Cohen-Sfady, M., Nussbaum, G., Pevsner-Fischer, M., Mor, F., Carmi, P., Zanin-Zhorov, A., Lider, O., Cohen, I.R., 2005. Heat shock protein 60 activates B cells via the TLR4-MyD88 pathway. J. Immunol. 175, 3594-3602.

De Nicola, M., Gattia, D., Bellucci, S., De Bellis, G., Micciulla, F., Pastore, R., Tiberia, A., Cerella, C., D Alessio, M., Antisari, M., 2007. Effect of different carbon nanotubes on cell viability and proliferation. J. Phys. Cond. Matt. 19, 395013-395019.

Donnet, J., Bansal, R., Wang, M. 1993. Carbon black: science and technology, second ed. Dekker, New York.

Duthie, S.J., Mavrommatis, Y., Rucklidge, G., Reid, M., Duncan, G., Moyer, M.P., Pirie, L.P., Bestwick, C.S., 2008. The response of human colonocytes to folate deficiency in vitro: functional and proteomic analyses. J. Proteome Res. 7, 3254-3266.

Endo, M., 1988. Grow carbon fibers in the vapor phase. Chem. Tech. 18, 568-576.

Endo, M., Strano, M., Ajayan, P., 2008. Potential applications of carbon nanotubes. Carbon Nanotubes 111, 13-61.

Flahaut, E., Durrieu, M.C., Remy-Zolghadri, M., Bareille, R., Baquey, C., 2006. Investigation of the cytotoxicity of CCVD carbon nanotubes towards human umbilical vein endothelial cells. Carbon 44, 1093-1099.

Gulumian, M., van Wyk, J.A., 1987. Hydroxyl radical production in the presence of fibres by a Fenton-type reaction. Chem. Biol. Interact. 62, 89-97.

Guo, L., Morris, D., Liu, X., Vaslet, C., Hurt, R., Kane, A., 2007. Iron bioavailability and redox activity in diverse carbon nanotube samples. Chem. Mater. 19, 3472-3478.

Guo, L., Von Dem Bussche, A., Buechner, M., Yan, A., Kane, A.B., Hurt, R.H., 2008. Adsorption of essential micronutrients by carbon nanotubes and the implications for nanotoxicity testing. Small 4, 721-727.

Haniu, H., Komori, N., Takemori, N., Singh, A., Ash, J.D., Matsumoto, H., 2006. Proteomic trajectory mapping of biological transformation: Application to developmental mouse retina. Proteomics 6, 3251-3261.

Haniu, H., Matsuda, Y., Takeuchi, K., 2009. Potential of a novel safety evaluation of nanomaterials using a proteomic approach. J. Health Sci. 55.

Herzog, E., Byrne, H.J., Casey, A., Davoren, M., Lenz, A.G., Maier, K.L., Duschl, A., Oostingh, G.J., 2009. SWCNT suppress inflammatory mediator responses in human lung epithelium in vitro. Toxicol. Appl. Pharmacol. 234, 378-390.

Hirano, S., Kanno, S., Furuyama, A., 2008. Multi-walled carbon nanotubes injure the plasma membrane of macrophages. Toxicol. Appl. Pharmacol. 232, 244-251.

Hod, Y., 2004. Differential control of apoptosis by DJ-1 in prostate benign and cancer cells. J. Cell Biochem. 92, 1221-1233.

Inoue, K., Takano, H., Koike, E., Yanagisawa, R., Sakurai, M., Tasaka, S., Ishizaka, A., Shimada, A., 2008. Effects of pulmonary exposure to carbon nanotubes on lung and systemic inflammation with coagulatory disturbance induced by lipopolysaccharide in mice. Exp. Biol. Med. 233, 1583-1590.

Jacobsen, N.R., Pojana, G., White, P., Moller, P., Cohn, C.A., Korsholm, K.S., Vogel, U., Marcomini, A., Loft, S., Wallin, H., 2008. Genotoxicity, cytotoxicity, and reactive oxygen species induced by single-walled carbon nanotubes and C(60) fullerenes in the FE1-Mutatrade markMouse lung epithelial cells. Environ. Mol. Mutagen. 49, 476-487.

Jiang, L., Zhong, Y., Akatsuka, S., Liu, Y.T., Dutta, K.K., Lee, W.H., Onuki, J., Masumura, K., Nohmi, T., Toyokuni, S., 2006. Deletion and single nucleotide substitution at G:C in the kidney of gpt delta transgenic mice after ferric nitrilotriacetate treatment. Cancer Sci. 97, 1159-1167.

Jin, H., Heller, D.A., Sharma, R., Strano, M.S., 2009. Size-dependent cellular uptake and expulsion of single-walled carbon nanotubes: single particle tracking and a generic uptake model for nanoparticles. ACS Nano 3, 149-158.

Kagan, V.E., Tyurina, Y.Y., Tyurin, V.A., Konduru, N.V., Potapovich, A.I., Osipov, A.N., Kisin, E.R., Schwegler-Berry, D., Mercer, R., Castranova, V., Shvedova, A.A., 2006. Direct and indirect effects of single walled carbon nanotubes on RAW 264.7 macrophages: role of iron. Toxicol. Lett. 165, 88-100.

Kostarelos, K., 2008. The long and short of carbon nanotube toxicity. Nat. Biotechnol. 26, 774-776.

Kubo, S., Hattori, N., Mizuno, Y., 2006. Recessive Parkinson's disease. Mov. Disord. 21, 885-893.

Le Naour, F., Misek, D.E., Krause, M.C., Deneux, L., Giordano, T.J., Scholl, S., Hanash, S.M., 2001. Proteomics-based identification of RS/DJ-1 as a novel circulating tumor antigen in breast cancer. Clin. Cancer Res. 7, 3328-3335.

Lippmann, M., 1990. Effects of fiber characteristics on lung deposition, retention, and disease. Environ. Health Perspect. 88, 311-317.

Liu, X., Guo, L., Morris, D., Kane, A.B., Hurt, R.H., 2008. Targeted removal of bioavailable metal as a detoxification strategy for carbon nanotubes. Carbon 46, 489-500.

MacKeigan, J.P., Clements, C.M., Lich, J.D., Pope, R.M., Hod, Y., Ting, J.P., 2003. Proteomic profiling drug-induced apoptosis in non-small cell lung carcinoma: identification of RS/DJ-1 and RhoGDIalpha. Cancer Res. 63, 6928-6934.

Monteiro-Riviere, N.A., Nemanich, R.J., Inman, A.O., Wang, Y.Y., Riviere, J.E., 2005. Multi-walled carbon nanotube interactions with human epidermal keratinocytes. Toxicol. Lett. 155, 377-384.

Muller, J., Huaux, F., Moreau, N., Misson, P., Heilier, J.F., Delos, M., Arras, M., Fonseca, A., Nagy, J.B., Lison, D., 2005. Respiratory toxicity of multi-wall carbon nanotubes. Toxicol. Appl. Pharmacol. 207, 221-231.

Nel, A., Xia, T., Madler, L., Li, N., 2006. Toxic potential of materials at the nanolevel. Science 311, 622-627.

Oberlin, A., Endo, M., Koyama, T., 1976. Filamentous growth of carbon through benzene decomposition. J. Cryst. Growth 32, 335-349.

Osterloh, A., Kalinke, U., Weiss, S., Fleischer, B., Breloer, M., 2007. Synergistic and differential modulation of immune responses by Hsp60 and lipopolysaccharide. J. Biol. Chem. 282, 4669-4680.

Petrak, J., Myslivcova, D., Man, P., Cmejla, R., Cmejlova, J., Vyoral, D., 2006. Proteomic analysis of iron overload in human hepatoma cells. Am. J. Physiol. Gastrointest. Liver Physiol. 290, G1059-G1066.

Poland, C.A., Duffin, R., Kinloch, I., Maynard, A., Wallace, W.A., Seaton, A., Stone, V., Brown, S., Macnee, W., Donaldson, K., 2008. Carbon nanotubes introduced into the abdominal cavity of mice show asbestos-like pathogenicity in a pilot study. Nat. Nanotechnol. 3, 423-428.

Pulskamp, K., Diabate, S., Krug, H.F., 2007. Carbon nanotubes show no sign of acute toxicity but induce intracellular reactive oxygen species in dependence on contaminants. Toxicol. Lett. 168, 58-74.

Sarkar, S., Sharma, C., Yog, R., Periakaruppan, A., Jejelowo, O., Thomas, R., Barrera, E.V., Rice-Ficht, A.C., Wilson, B.L., Ramesh, G.T., 2007. Analysis of stress responsive genes induced by single-walled carbon nanotubes in BJ Foreskin cells. J. Nanosci. Nanotechnol. 7, 584-592.

Shvedova, A.A., Fabisiak, J.P., Kisin, E.R., Murray, A.R., Roberts, J.R., Tyurina, Y.Y., Antonini, J.M., Feng, W.H., Kommineni, C., Reynolds, J., Barchowsky, A., Castranova, V., Kagan, V.E., 2008. Sequential exposure to carbon nanotubes and bacteria enhances pulmonary inflammation and infectivity. Am. J. Respir. Cell Mol. Biol. 38, 579-590.

Shvedova, A.A., Kisin, E.R., Murray, A.R., Gorelik, O., Arepalli, S., Castranova, V., Young, S.H., Gao, F., Tyurina, Y.Y., Oury, T.D., Kagan, V.E., 2007. Vitamin E deficiency enhances pulmonary inflammatory response and oxidative stress induced by single-walled carbon nanotubes in C57BL/6 mice. Toxicol. Appl. Pharmacol. 221, 339-348.

Shvedova, A.A., Kisin, E.R., Murray, A.R., Kommineni, C., Castranova, V., Fadeel, B., Kagan, V.E., 2008. Increased accumulation of neutrophils and decreased fibrosis

in the lung of NADPH oxidase-deficient C57BL/6 mice exposed to carbon nanotubes. Toxicol. Appl. Pharmacol. 231, 235-240.

Soto, K., Garza, K.M., Murr, L.E., 2007. Cytotoxic effects of aggregated nanomaterials. Acta Biomater. 3, 351-358.

Takagi, A., Hirose, A., Nishimura, T., Fukumori, N., Ogata, A., Ohashi, N., Kitajima, S., Kanno, J., 2008. Induction of mesothelioma in p53+/- mouse by intraperitoneal application of multi-wall carbon nanotube. J. Toxicol. Sci. 33, 105-116.

Usui, Y., Aoki, K., Narita, N., Murakami, N., Nakamura, I., Nakamura, K., Ishigaki, N., Yamazaki, H., Horiuchi, H., Kato, H., Taruta, S., Kim, Y.A., Endo, M., Saito, N., 2008. Carbon nanotubes with high bone-tissue compatibility and bone-formation acceleration effects. Small 4, 240-246.

Warheit, D.B., 2006. What is currently known about the health risks related to carbon nanotube exposures? Carbon 44, 1064-1069.

Witzmann, F.A., Monteiro-Riviere, N.A., 2006. Multi-walled carbon nanotube exposure alters protein expression in human keratinocytes. Nanomedicine 2, 158-168.

Wood-Kaczmar, A., Gandhi, S., Wood, N.W., 2006. Understanding the molecular causes of Parkinson's disease. Trends Mol. Med. 12, 521-528.

Yang, H., Liu, C., Yang, D., Zhang, H., Xi, Z., 2009. Comparative study of cytotoxicity, oxidative stress and genotoxicity induced by four typical nanomaterials: the role of particle size, shape and composition. J. Appl. Toxicol. 29, 69-78.

Yang, S.T., Wang, X., Jia, G., Gu, Y., Wang, T., Nie, H., Ge, C., Wang, H., Liu, Y., 2008. Long-term accumulation and low toxicity of single-walled carbon nanotubes in intravenously exposed mice. Toxicol. Lett. 181, 182-189.

Figure Legends

Figure 1. Proliferation of U937 cells. U937 cells (5×10^4 cells/ml) were exposed to three grades of MWCNTs (0.1 mg/ml) for 96 h. The cells were stained with trypan blue and counted at 24-h intervals. $n = 4$. *$p < 0.05$.

Figure 2. Cytotoxicity of MWCNTs. U937 cells stained with 0.4% trypan blue at 48 h. (a) Control, (b) as-grown, (c) HTT1800, and (d) HTT2800.

Figure 3. Two-DE gels. (a) Control, (b) HTT1800, and (c) HTT2800. Numbered spots were changed by over two-fold with statistically significant differences ($p < 0.05$) in HTT1800 or HTT2800 compared to the control. $n = 4$.

Figure
Click here to download high resolution image

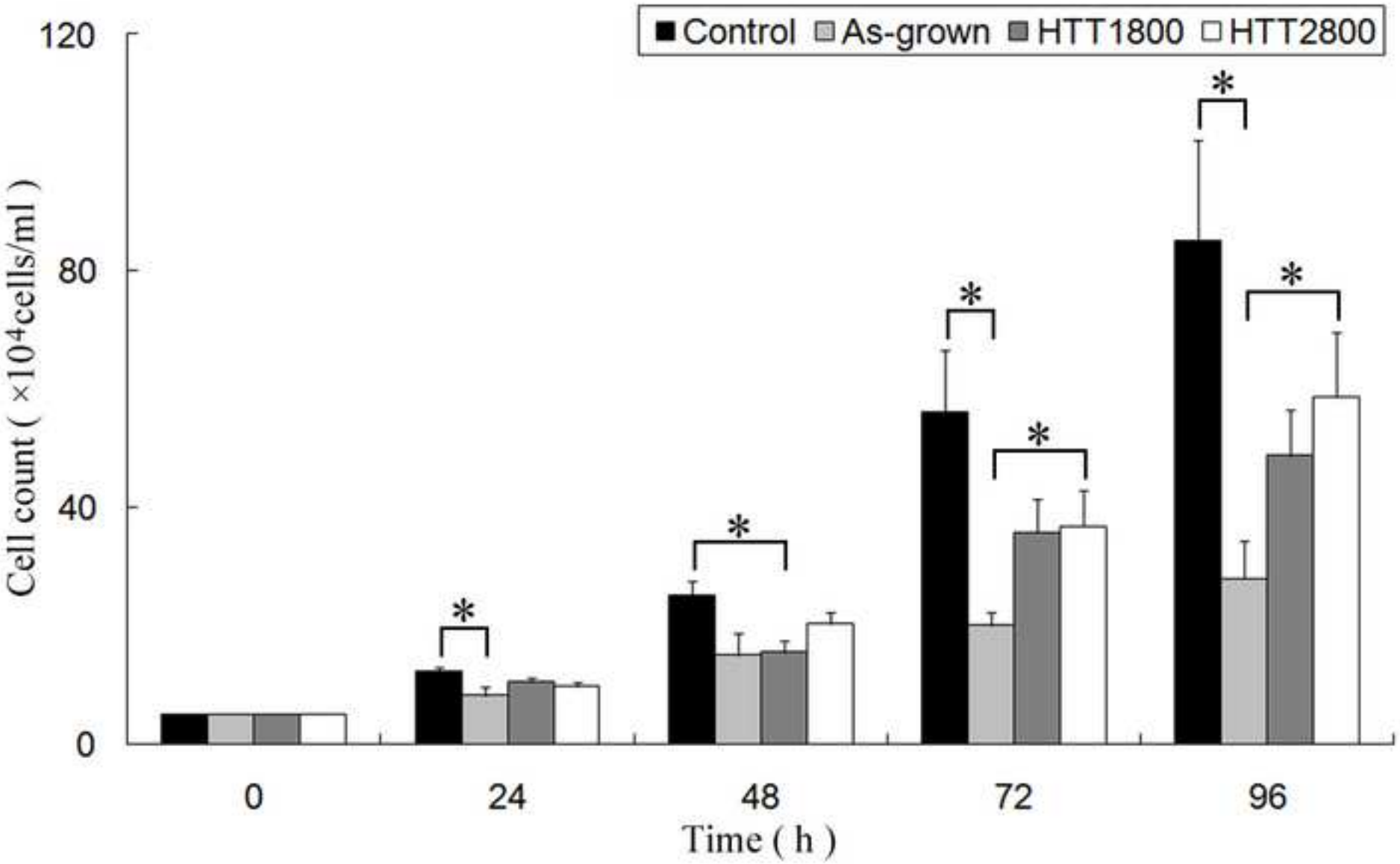

Figure

Click here to download high resolution image

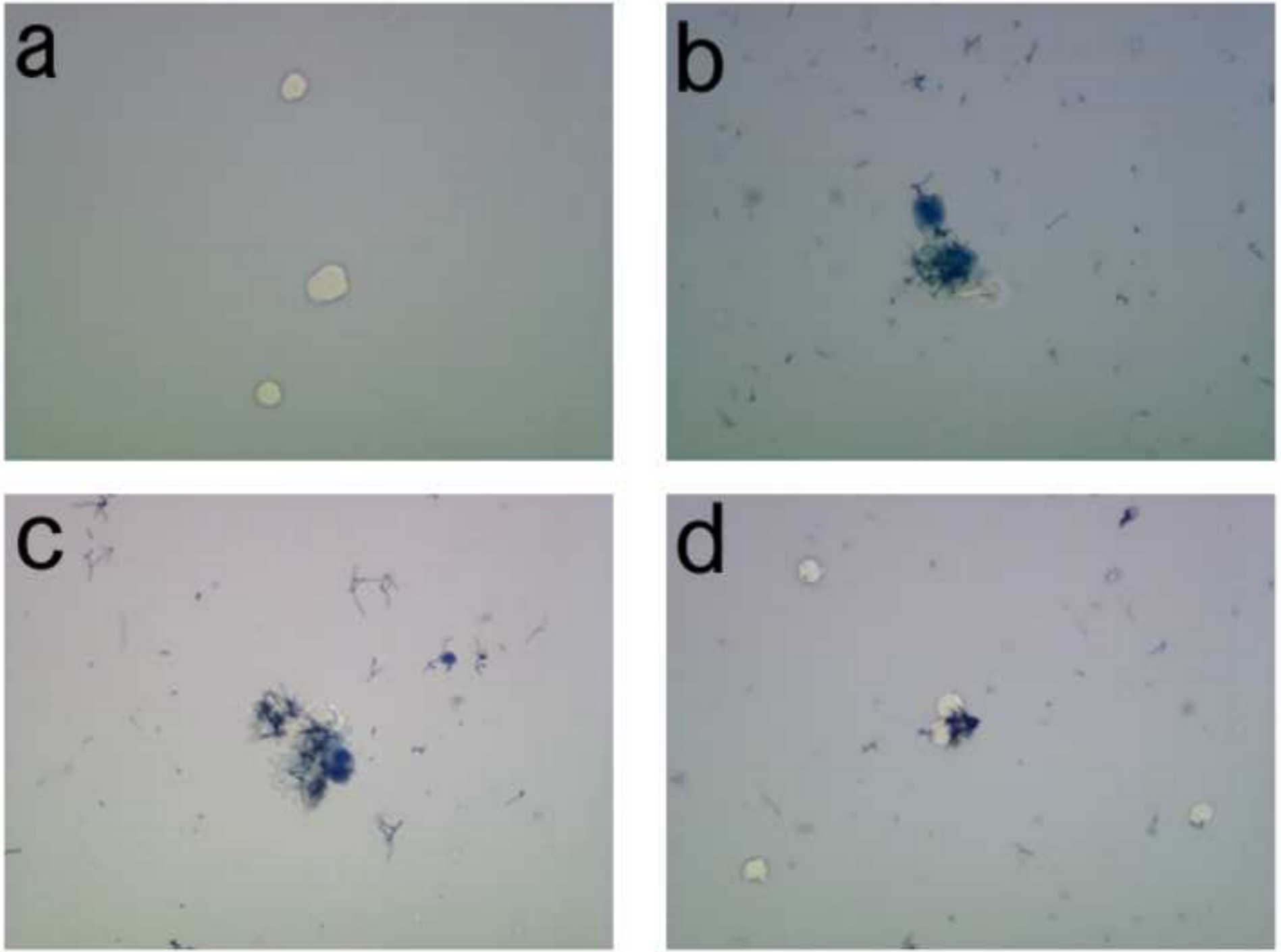

Figure

Click here to download high resolution image

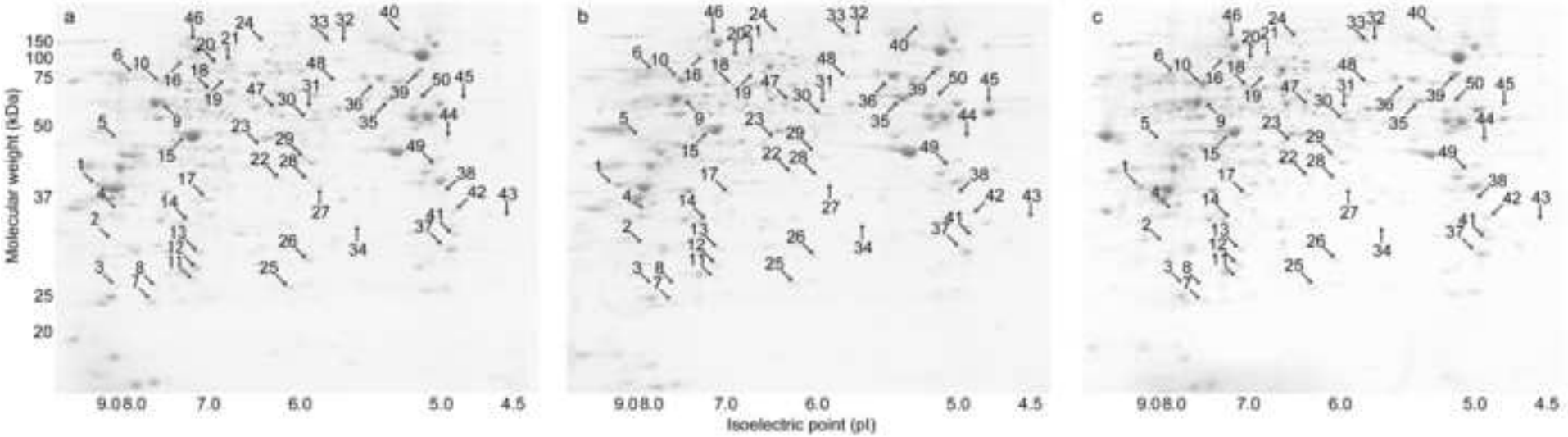

Table 1. Basic properties of multi-walled carbon nanotubes

	As-grown	HTT1800	HTT2800	Testing method
Diameter (nm)	100-150	100-150	100-150	FE-SEM
Length (μm)	10-20	10-20	10-20	FE-SEM
d_{002} (Å)	-	-	0.339	X-ray diffraction
R value (I_d/I)[a]	1.041	0.855	0.051	Raman spectroscopy
Specific surface area (m^2/g)	-	26	13	N_2 adsorption
Real density (g/cm^3)	-	-	2.09	Pycnometer
Iron content (ppm)	12,000	80	<20	ICP-MS
Soluble iron content (%)[b]	0	91	100	ICP-MS
Polycyclic aromatic hydrocarbons (wt%)[c]	0.19	None	None	GC-MS spectroscopy
Oxidation temperature (^oC)[d]	630	720	820	TGA

a R refers to the intensity of D band over the intensity of G band.

b We have determined the dissolved amount of iron by refluxing 5 g of nanotubes in hydrochloric acid (0.6 N) for 25 h.

c We have measured acetone-soluble components.

d We have determined the oxidation temperatures via the derivation of TGA curve.

Table 2 Identified proteins

spot No.	Protein Name	Theoritical MW	Theoritical pI	MOWSE Score	Coverage	Ratio HTT 1800	Ratio HTT 2800	SwissProt Accession No.
1	heterogeneous nuclear ribonucleoprotein	37478	8.97	141	43%	* 2.12	# 1.45	P22626
2	small nuclear ribonucleoprotein polypeptide A'	28540	8.72	97	29%	* 0.23	0.55	P09661
3	proteasome subunit β type-1	26757	8.27	82	27%	* 0.36	# 0.59	P20618
4	annexin A2	38864	7.57	114	28%	* 3.58	2.50	P07355
5	vasodilator-stimulated phosphoprotein	39977	9.05	78	24%	* 3.20	1.58	P50552
6	heterogeneous nuclear ribonucleoprotein M	77819	8.84	186	32%	* 2.01	1.25	P52272
7	phosphatidylethanolamine-binding protein 1	21186	7.01	107	45%	* 0.35	* 0.44	P30086
8	flavin reductase	22248	7.13	74	40%	* 0.13	0.42	P30043
9	pyruvate kinase isozymes M1/M2	58664	7.60	129	16%	* 2.62	1.29	P14618
10	transketolase	68687	7.58	242	30%	* 2.22	1.84	P29401
11	proteasome subunit α type-2	26024	6.92	76	17%	* 0.47	0.56	P25787
12	triosephosphate isomerase	27008	6.45	134	42%	* 0.43	* 0.45	P60174
13	phosphoglycerate mutase 1	28928	6.67	84	20%	* 0.49	# 0.51	P18669
14	actin related protein 2/3 complex subunit 2	34454	6.84	72	19%	0.59	* 0.50	O15144
15	6-phosphogluconate dehydrogenase, decarboxylating	53745	6.80	71	12%	0.58	* 0.49	P52209
16	far upstream element-binding protein 2	73542	6.84	140	22%	* 2.35	2.06	Q92945
17	cytosolic malate dehydrogenase	36687	6.91	87	20%	* 0.49	# 0.65	P40925
18	lamin A/C	65167	6.40	193	34%	1.73	* 2.47	P02545
19	mitochondrial import receptor subunit	68264	6.75	69	12%	* 2.34	1.81	O94826
20	polyribonucleotide nucleotidyltransferase 1	86664	7.87	86	13%	* 2.32	1.82	Q8TCS8
21	δ-1-pyrroline-5-carboxylate synthetase	88171	6.66	87	9%	* 2.10	# 1.79	P54886
22	transaldolase	37730	6.36	167	36%	* 0.45	0.58	P37837
23	squalene synthetase	48724	6.10	68	17%	* 0.47	0.65	P37268
24	α-ketoglutarate dehydrogenase	117353	6.40	119	12%	* 4.13	* 4.10	Q02218
25	protein DJ-1	20092	6.33	114	43%	* 0.42	* 0.35	Q99497
26	heat shock protein β-1	22840	5.98	90	26%	# 0.59	* 0.42	P04792
27	transaldolase 1	37730	6.36	150	29%	* 0.35	0.46	P37837
28	serine/threonine-protein phosphatase PP1-α catalytic subunit	38411	5.94	120	34%	# 0.52	* 0.29	P62136
29	leukocyte elastase inhibitor	42857	5.90	133	32%	0.65	* 0.48	P30740
30	serine/threonine-protein phosphatase 2A 55 kDa regulatory subunit B α isoform	52299	5.82	103	16%	0.72	* 0.49	P63151
31	interferon-induced protein 53	49247	6.03	76	10%	* 0.43	0.80	P23381
32	DNA mismatch repair protein Msh2	105600	5.58	69	10%	* 3.13	* 3.78	P43246
33	neutral α-glucosidase AB	107375	5.74	183	19%	* 3.09	* 3.05	Q14697
34	F-actin capping protein subunit β	31036	5.69	104	26%	* 0.36	0.42	P47756
35	heat shock protein 60	61229	5.70	172	28%	* 2.70	1.43	P10809
36	lamin-B2	67790	5.29	183	31%	* 2.44	1.71	Q03252
37	14-3-3 protein γ	28498	4.80	150	36%	# 0.50	* 0.48	P61981
38	elongation factor 1-δ	31245	4.90	124	34%	0.33	* 0.18	P29692
39	78 kDa glucose-regulated protein	72431	5.07	176	27%	* 2.33	1.27	P11021
40	DNA damage-binding protein 1	128470	5.16	84	7%	2.10	* 2.82	Q16531
41	14-3-3 protein ε	29369	4.63	150	43%	* 0.41	0.59	P62258
42	proliferating cell nuclear antigen	29177	4.57	115	28%	* 0.47	0.63	P12004
43	splicing factor SC35	25461	11.86	100	38%	* 0.27	0.30	Q01130
44	ribonuclease inhibitor	52214	4.71	68	15%	* 0.44	0.61	P13489
45	calreticulin	48325	4.29	68	13%	* 4.88	1.52	P27797

*$p < 0.05$ and more than 2-fold change, # $p < 0.05$ only

Table 3 Functions of classified proteins

Nucleobase, nucleoside, nucleotide and nucleic acid metabolic process
small nuclear ribonucleoprotein polypeptide A', heat shock protein 60, proliferating cell nuclear antigen, ribonuclease inhibitor, phosphoglycerate mutase 1*, heterogeneous nuclear ribonucleoprotein A2/B1*, interferon-induced protein 53, calreticulin, transaldolase, cytosolic malate dehydrogenase*, DNA mismatch repair protein Msh2*, 6-phosphogluconate dehydrogenase decarboxylating#, heterogeneous nuclear ribonucleoprotein M, triosephosphate isomerase*, splicing factor SC35, DNA damage-binding protein 1#, polyribonucleotide nucleotidyltransferase 1, far upstream element-binding protein 2
Protein metabolic process
actin related protein 2/3 complex subunit 2#, heat shock protein β-1*, heat shock protein 60, proteasome subunit β type-1*, calreticulin, interferon-induced protein 53, proteasome subunit α type-2, elongation factor 1-δ#, F-actin capping protein subunit β, 14-3-3 protein epsilon, serine/threonine-protein phosphatase PP1-α catalytic subunit*, serine/threonine-protein phosphatase 2A 55 kDa regulatory subunit B α isoform#, DNA damage-binding protein 1#
Catalytic process
ribonuclease inhibitor, pyruvate kinase isozymes M1/M2, phosphoglycerate mutase 1*, proteasome subunit β type-1*, proteasome subunit α type-2, transaldolase, cytosolic malate dehydrogenase*, 6-phosphogluconate dehydrogenase decarboxylating#, triosephosphate isomerase*, α-ketoglutarate dehydrogenase*, DNA damage-binding protein 1#, polyribonucleotide nucleotidyltransferase 1
Biosynthetic process
heat shock protein β-1*, proliferating cell nuclear antigen, interferon-induced protein 53, calreticulin, elongation factor 1-δ#, squalene synthetase, DNA mismatch repair protein Msh2*, 6-phosphogluconate dehydrogenase decarboxylating#, δ-1-pyrroline-5-carboxylate synthetase*, triosephosphate isomerase*
Signal transduction/cell communication
heat shock protein 60, 78 kDa glucose-regulated protein, proliferating cell nuclear antigen, calreticulin, elongation factor 1-δ#, DNA mismatch repair protein Msh2*, 14-3-3 protein γ*, 14-3-3 protein ε, serine/threonine-protein phosphatase 2A 55 kDa regulatory subunit B α isoform#, protein DJ-1*
Multicellular organismal development
annexin A2, heat shock protein 60, ribonuclease inhibitor, calreticulin, DNA mismatch repair protein Msh2*, triosephosphate isomerase*, 14-3-3 protein γ*, serine/threonine-protein phosphatase PP1-α catalytic subunit*, 14-3-3 protein ε
Carbohydrate metabolic process
pyruvate kinase isozymes M1/M2, phosphoglycerate mutase 1*, transaldolase, cytosolic malate dehydrogenase*, 6-phosphogluconate dehydrogenase decarboxylating#, triosephosphate isomerase*, serine/threonine-protein phosphatase PP1-α catalytic subunit*, α-ketoglutarate dehydrogenase*, neutral α-glucosidase AB*
Response to stress
heat shock protein β-1*, annexin A2, heat shock protein 60, 78 kDa glucose-regulated protein, proliferating cell nuclear antigen, DNA mismatch repair protein Msh2*, DNA damage-binding protein 1#, protein DJ-1
Transport
mitochondrial import receptor subunit TOM70, proliferating cell nuclear antigen, heterogeneous nuclear ribonucleoprotein A2/B1*, calreticulin, 14-3-3 protein γ*, 14-3-3 protein ε, far upstream element-binding protein 2, protein DJ-1
Cell differentiation
heat shock protein β-1*, heat shock protein 60, 78 kDa glucose-regulated protein, calreticulin, DNA mismatch repair protein Msh2*, 14-3-3 protein γ*, 14-3-3 protein ε
Cell cycle
proteasome subunit β type-1*, proteasome subunit α type-2, calreticulin, DNA mismatch repair protein Msh2*, serine/threonine-protein phosphatase PP1-α catalytic subunit*, DNA damage-binding protein 1#
Cell death
heat shock protein β-1*, heat shock protein 60, 78 kDa glucose-regulated protein, calreticulin, DNA mismatch repair protein Msh2*
Organelle organization and biogenesis
actin related protein 2/3 complex subunit 2#, mitochondrial import receptor subunit TOM70, calreticulin, DNA mismatch repair protein Msh2*, F-actin capping protein subunit β
Translation
heat shock protein β-1*, interferon-induced protein 53, calreticulin, elongation factor 1-δ#
Cell proliferation
heat shock protein 60, proliferating cell nuclear antigen, interferon-induced protein 53, calreticulin
Transcription
calreticulin, far upstream element-binding protein 2
Lipid metabolic process
squalene synthetase, triosephosphate isomerase*

*$p < 0.05$ in HTT1800 and HTT2800 compared to control

# $p < 0.05$ in HTT2800 only compared to control